

Received 14 September 2023, accepted 27 September 2023, date of publication 2 October 2023, date of current version 11 October 2023.

Digital Object Identifier 10.1109/ACCESS.2023.3321371

RESEARCH ARTICLE

Energy Price-Based Resource Scheduling for Network Lifetime Extending in Cooperative D2D Communications Overlaying Cellular Networks

YANG YU¹ AND XIAOQING TANG²

¹Electronic Information School, Hubei Three Gorges Polytechnic, Yichang 443000, China

²School of Artificial Intelligence, Hubei University, Wuhan 430062, China

Corresponding author: Yang Yu (yuyang@tgc.edu.cn)

This work was supported in part by the Research Platform Construction Project of Hubei Three Gorges Polytechnic under Grant 2023KYPT0201, and in part by the Natural Science Foundation of Hubei Province under Grant 2022CFB840.


ABSTRACT This paper considers device-to-device (D2D) communications overlaying cellular networks. Combined with cooperative relay technology, a D2D user can serve as a relay for a cellular link and gain the opportunity to access the corresponding cellular spectrum. Considering mobile terminals' limited battery capacity and motivated by green communication, we propose a resource scheduling scheme, which comprises joint power and spectrum allocation, mode selection, and link matching. Unlike previous works, to balance energy utilization and extend the network lifetime, this scheme sets a price for each node and minimizes the system cost during each frame instead of energy efficiency (EE). Specifically, we investigate the power and spectrum allocation problem to characterize the minimum cost of matched links. We prove it to be nonconvex and obtain the optimal solution by the graphic method and Newton's method with a small number of iterations. We also discuss the energy pricing strategy. In order to reduce communication and computation overhead, we propose a heuristic pricing strategy that involves no iteration and supposes nodes' energy prices are inversely proportional to their residual energy. Through simulations under various cases, we verify that the proposed scheme significantly improves network lifetime and suits real-time operations while guaranteeing the quality of service (QoS) requirement. Moreover, the simulation results demonstrate that the proposed scheme performs the same as the maximum EE scheme if the energy prices are equal at each node.

INDEX TERMS Cooperative D2D communication, energy price, green communication, network lifetime, resource scheduling.

I. INTRODUCTION

With the rapid development of wireless communications at the industrial and technological levels, mobile terminals and data traffic have shown explosive growth in the past twenty years. As a result, spectrum resources are becoming increasingly crowded and scarce. To improve the spectral efficiency (SE) of wireless communication systems, a series of key technologies have emerged, such as heterogeneous network [1], massive multiple-input multiple-output (MIMO) [2],

device-to-device (D2D) communication [3]. Among them, D2D communication refers to the technology that allows direct communication between user equipment (UE) with or without the involvement of network infrastructures such as a base station (BS) or an access point [4]. Since mobile users' high data rate services (e.g., video sharing, gaming) in cellular networks are potentially in range for direct communications, D2D communications can improve the system SE. Moreover, D2D communication can also reduce latency, improve energy efficiency (EE), and reduce cellular data service load through direct communication, thereby avoiding system congestion [5]. In general, D2D links reuse

The associate editor coordinating the review of this manuscript and approving it for publication was Miguel López-Benítez .

cellular spectrum resources, and there are generally two reuse modes: underlay and overlay.

Cooperative relay technologies can improve the link quality of wireless networks by achieving spatial diversity advantages [6]. In the context of overlay D2D communications, D2D users can serve as relays for cellular users (CUs) and gain a higher opportunity to access the cellular spectrum band. On the other hand, CUs can improve their performance by D2D users relaying their traffic. It will achieve a win-win situation for both sides to cooperate. Based on the above analysis, the authors of [7] first proposed a cooperative D2D communication framework for cellular networks, where D2D receivers (DRs) served as relays.

Effective resource scheduling enables high performance for both cellular and D2D links. As motivated, resource scheduling in cooperative D2D communication has been widely investigated towards different performance metrics and under various mathematical frameworks. The authors in [8] investigated the pairing problem among multiple CUs and D2D links under the cooperative D2D communication framework presented in [7], formulated it as a one-to-one matching game, and then proposed a learning algorithm to solve it. Further, in [9], they proposed a two-timescale scheduling allocation scheme to reduce the overhead under the previous matching model. In [10], Lee et al. investigated cooperative D2D communication in an uplink cellular network. They derived the optimal resource allocation scheme to maximize the average achievable rate under the outage probability constraint. Based on contract theory, the authors of [11] proposed a cooperative spectrum-sharing mechanism to increase transmission opportunities for the D2D links while maximizing the profit of the cellular links. The authors of [12] developed an optimal power allocation scheme to maximize the sum rate of non-orthogonal multiple access (NOMA)-based D2D communications with imperfect successive interference cancellation (SIC) decoding. In [13], Gao et al. investigated the optimal dynamic social-aware peer selection with spectrum-power trading to maximize the average sum EE of CUs in D2D-enabled uplink orthogonal frequency division multiple access (OFDMA) cellular networks. Most of the above literature focuses on improving UEs' transmission rate, ignoring their energy consumption (EC). Some of them, e.g., [13], emphasize maximizing EE for CUs or D2D users, not the entire network.

Due to battery capacity limitations and the exponentially increasing demand for mobile traffic, EE has become a critical system metric that leads to green communication [14]. Considering that most wireless communication networks are energy-limited, resource scheduling strategies that maximize system throughput will lead to the rapid EC of network nodes and the consequent frequent replacement of batteries, contrary to the principle of green communication. Many existing works have focused on designing and operating energy-efficient D2D-enabled networks, including but not limited to the cooperative D2D communication framework. In [15], the authors investigated the SE and EE tradeoff

relationship and proposed a distributed energy-efficient resource allocation scheme by exploiting the properties of nonlinear fractional programming. In [16], considering the limited computation resources, Cheng et al. proposed a D2D-assisted computation offloading scheme, in which the block coordinate descent method combined with the successive convex approximation is employed to maximize the EE of NOMA-enabled cognitive radio networks. The authors of [17] derived an energy-efficient resource allocation scheme for D2D communications underlying NOMA-based cellular networks with energy harvesting. The proposed scheme could maximize the EE of a D2D link while guaranteeing the quality of service (QoS) of CUs with low complexity. In addition, deep learning applications on resource scheduling have recently attracted much attention because they handle nonconvex optimization problems with a low computation time [18]. The authors in [19] applied a learning-based method to maximize both SE and EE for wireless-powered D2D networks. In [20] and [21], reinforcement-learning methods addressed energy-efficient resource allocation by making agents interact with unknown wireless environments.

Green communication aims to explore sustainability regarding environmental conditions and EC without compromising users' QoS. Most of the literature, including the ones mentioned above, currently focuses on improving the EE of D2D-enabled cellular networks. However, compared to solely maximizing EE, it is more important to minimize the labor costs required for network maintenance and extend the lifetime of these networks for green communication [22]. Therefore, to extend the network lifetime, it is necessary to reduce the EC during each transmission period and balance the utilization of each UE's residual energy while guaranteeing UEs' QoS requirements.

According to price theory, the price of a commodity reflects its supply and demand relationship. In short, if the price of a commodity is relatively high, its supply/demand ratio is relatively small, and vice versa [23]. Following this idea, we price each UE's residual energy and schedule system wireless resources according to minimum cost criteria during each frame. Guiding by a reasonable pricing mechanism, the EC among different nodes will be balanced, and the network lifetime will be extended. There are many existing works related to price setting [8], [9], [11], [13], [24], [25], [26]. According to our perspective, there are three issues with them. Firstly, to the best of our knowledge, they have rarely focused on balancing UEs' EC in cooperative D2D communications to prolong the network lifetime. Take [24] as an example. It proposed a spectrum-power trading scheme to maximize the weighted sum EE of D2D links for cooperative D2D overlaying communications. However, the weights of the D2D links were predefined and maintained constants rather than dynamically adjusting according to their residual energy. Besides, the EC of CUs was not considered. Similarly, the author of [13] adopted the average EEs of CUs as the utility function, which implied the weights of the CUs were equal.

Secondly, one user's utility function comprises gain and loss, usually measured by two performance metrics. How to set prices to link them is a problem. Existing works have designed various utility functions [27], introduced extra auxiliary parameters, and set these parameters as constants for simplicity to tackle this problem. For instance, [25] formulated the joint bandwidth allocation and relay selection problem in multi-homing cooperative D2D networks as a two-stage Stackelberg game. Except for the charging price vector \mathbf{P} , the authors also introduced α as the unit cost per bit into the utility in (11) to link the gain and loss. Then, they set $\alpha = 1$ for the benefit of simplicity. The same situation also occurred in [26]. Besides the price λ_i , the authors introduced transmission rate income and payoff factors in users' utility and set them as constants. Some other works even set the prices as constants [9]. From an intuitive perspective, these assumptions and simplifications differ from actual economic activities and lack convincingness.

Lastly, most existing works set prices through iterative methods, which would introduce additional communication and computation overheads, such as the pricing algorithm in [24] and [26]. Based on the above analysis, we are naturally motivated to develop a pricing algorithm that does not require iteration and is only related to UEs' residual energy.

Meanwhile, many existing studies investigate resource allocation problems between the cellular and D2D links based on certain simplified conditions. For example, the authors of [7] considered resource scheduling for cooperative D2D communications with fixed spectrum allocation. In [8] and [9], the authors assumed a D2D transmitter (DT) forwards a CU's data and communicates with a DR with the same transmit power. However, these simplified conditions constrain these schemes to achieve better performance.

This paper investigates the resource scheduling problem based on energy price for cooperative D2D communications overlaying cellular networks from the network-centric [28] perspective. The main contributions of this work are summarized as follows.

- 1) We present a resource scheduling scheme comprising jointly power and spectrum allocation, mode selection, and link matching. By introducing energy price, the proposed scheme optimizes the system cost function during the network lifetime instead of traditional EE to extend the network lifetime of our system. Numerical simulation results verify the superiority of the proposed scheme and show its efficiency.
- 2) We propose an optimal algorithm for solving the resource allocation problem without simplified conditions. Unlike [29], we prove this problem is nonconvex and divide it into two sub-problems, which can be solved by the graphic method and Newton's method, respectively. Furthermore, we show that its solution is optimal and can be obtained with low computational complexity through simulation.
- 3) We discuss the energy pricing strategy and propose a heuristic scheme that can balance the utilization of each

UE's energy and prolong the network lifetime. This scheme does not involve iteration, which can reduce computation overhead. Besides, if the energy prices are equal at each node during each frame, the BS does not need the feedback of energy state information. In this case, the simulation results demonstrate that the proposed scheme minimizes the overall system EC and performs the same as the maximum EE scheme in terms of EE. Moreover, it has a much lower computational complexity than the maximum EE scheme.

The rest of this paper is organized as follows. In Section II, we describe the considered system model. We study the network-centric optimal resource scheduling problem and the energy pricing strategy in Section III. Numerical results are presented in Section IV to demonstrate the benefits of our proposed schemes. Finally, we conclude this paper in Section V.

II. SYSTEM MODEL

We consider D2D communications overlaying an OFDMA-based cellular network. As shown in Fig. 1, a BS is located at the geographic center of a single cell and operates over an authorized spectrum band. The OFDMA technique divides the band into several orthogonal channels with equal bandwidth W . An OFDMA frame lasts T in the time domain. There are M cellular links and N D2D links in this cell. $\mathcal{M} = \{1, 2, \dots, M\}$ and $\mathcal{N} = \{1, 2, \dots, N\}$ denote the sets of the cellular links and the D2D links, respectively. The BS supports operator-controlled D2D communications [30], [31]. Due to the limited power budgets of mobile terminals, we focus on the uplink transmission, although the proposed system is also suitable for the case of the downlink transmission.

Remark 1: Since the 3rd generation partnership project (3GPP) release 15 was frozen, the fifth-generation (5G) new radio (NR) has adopted the orthogonal frequency division multiplexing (OFDM) for the enhanced mobile broadband (eMBB) scenario [32]. For simplicity in the discussion, we take the OFDMA-enabled D2D communication as an example to introduce the proposed scheme. The proposed scheme described in the next section can also be applied in NOMA-based uplink cellular networks for the massive machine-type communication (mMTC) scenario. Moreover, it also has the potential to combine with technologies beyond 5G, e.g., simultaneously transmitting and reflecting reconfigurable intelligent surface (STAR-RIS) [33], which we will explore in our future work.

At the beginning of each frame, the BS collects each link's channel status information (CSI) through channel probing and feedback for resource scheduling [34]. During one frame, each cellular link is assigned only one channel. The BS does not assign dedicated spectrum resources to the D2D links and allows them to share the channels of the cellular links through cooperative or overlay mode. In the cooperative mode, one D2D user serves as a relay for a cellular link. After the cellular link completes data transmission, the BS allows the D2D link to access the corresponding channel for its data transmission.

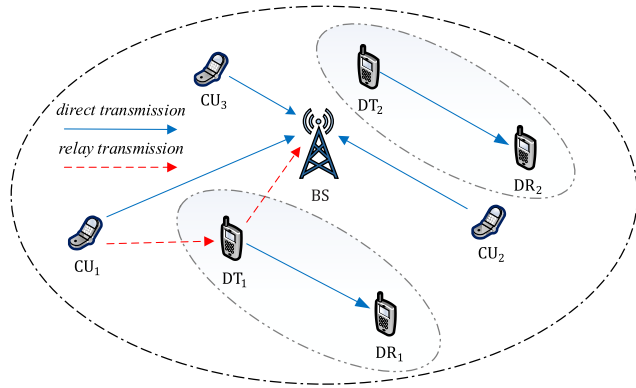


FIGURE 1. An illustration of the transmission in the cooperative and overlay modes.

TABLE 1. Summary of important notations.

Symbol	Definition
W	The channel bandwidth
T	The frame length
M	The number of the cellular links
N	The number of the D2D links
\mathcal{M}	The set of the cellular links
\mathcal{N}	The set of the D2D links
h_{mb}	The channel gain of the $CU_m \rightarrow BS$ link
h_{mn}	The channel gain of the $CU_m \rightarrow DT_n$ link
h_{nb}	The channel gain of the $DT_n \rightarrow BS$ link
h_{nn}	The channel gain of the $DT_n \rightarrow DR_n$ link
p_{mb}	The transmit power of CU_m
p_{nb}	The transmit power of DT_n for relaying data
p_{nn}	The transmit power of DT_n for its own data transmission
n_0	The additive white Gaussian noise power spectral density
θ_{mn}	The spectrum allocation factor for cellular link m and D2D link n in the cooperative mode
α_{mn}	The spectrum allocation factor for cellular link m and D2D link n in the overlay mode
μ_m	The energy price of CU_m
μ_n	The energy price of DT_n
Q_m	The minimum rate requirement of cellular link m
Q_n	The minimum rate requirement of D2D link n
ε_0	The iteration termination parameter for Newton's method
π	The mode selection and link matching strategy

Without loss of generality, we consider cases where DTs act as relays. For the sake of simplicity, we assume that the transmission directions of the D2D links remain unchanged during each frame. Fig. 1 illustrates the transmission between cellular link 1 and D2D link 1 in the cooperative mode, and the transmission between cellular link 2 and D2D link 2 in the overlay mode, respectively. Some important notations of this paper are presented in Table. 1.

The transmission in the cooperative mode between cellular link $m \in \mathcal{M}$ and D2D link $n \in \mathcal{N}$ during an OFDMA frame is divided into three phases, as shown in Fig. 2. In phase one, CU_m broadcasts its data toward the BS and DT_n with transmit power p_{mb} . In phase two, DT_n forwards the received data to the BS with transmit power p_{nb} . The signals from CU_m and DT_n are merged through the maximal-ratio combining (MRC) method at the BS [35]. Both phase one and phase

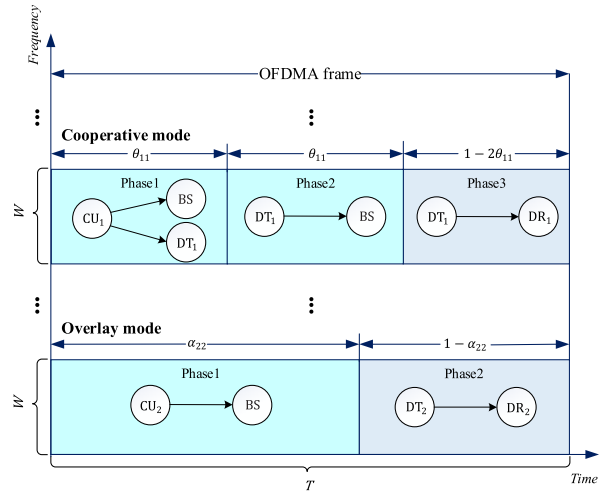


FIGURE 2. Frame structure of the cooperative D2D communication.

two last θ_{mn} of the frame length, where $\theta_{mn} \in (0, 0.5)$ is referred to as the spectrum allocation factor. Phase three lasts $1 - 2\theta_{mn}$ of the frame length, where DT_n transmits its data with power p_{nn} . The EC of CU_m in phase one is $\theta_{mn}p_{mb}T$. The EC of DT_n in the last two phases are $\theta_{mn}p_{nb}T$ and $(1 - 2\theta_{mn})p_{nn}T$, respectively. This paper takes the decode-and-forward (DF) protocol as an example and ignores the receivers' EC.

Assuming that channel gains remain constant during one frame, we denote $h_{mb}, h_{mn}, h_{nb}, h_{nn}$ as channel gains of the $CU_m \rightarrow BS$ link, the $CU_m \rightarrow DT_n$ link, the $DT_n \rightarrow BS$ link, and the $DT_n \rightarrow DR_n$ link, respectively. We define parameters $\lambda_{mb} \triangleq h_{mb}/(Wn_0)$, $\lambda_{mn} \triangleq h_{mn}/(Wn_0)$, $\lambda_{nb} \triangleq h_{nb}/(Wn_0)$ and $\lambda_{nn} \triangleq h_{nn}/(Wn_0)$, where n_0 denotes the Gaussian noise power spectral density. Then, the achievable rates of cellular link m and D2D link n during one frame can be written as

$$R_m = \theta_{mn}W \log_2 (1 + \min \{p_{mb}\lambda_{mn}, p_{mb}\lambda_{mb} + p_{nb}\lambda_{nb}\}), \quad (1)$$

$$R_n = (1 - 2\theta_{mn})W \log_2 (1 + p_{nn}\lambda_{nn}). \quad (2)$$

In the overlay mode, the BS reserves a part of a frame for D2D communication. Assuming that CU_m transmits for α_{mn} of the frame length, the EC of CU_m and DT_n can be denoted as $\alpha_{mn}p_{mb}T$ and $(1 - \alpha_{mn})p_{nn}T$, where $\alpha_{mn} \in (0, 1)$. The achievable rates of cellular link m and D2D link n during a frame can be expressed as

$$R_m = \alpha_{mn}W \log_2 (1 + p_{mb}\lambda_{mb}), \quad (3)$$

$$R_n = (1 - \alpha_{mn})W \log_2 (1 + p_{nn}\lambda_{nn}). \quad (4)$$

Remark 2: To schedule resources for M cellular and N D2D links, the BS must gather the instantaneous CSI of the links not directly involved with the BS through control channels at the beginning of each frame. Suppose a CSI report contains B bits. For the cooperative mode, the CSI of the $CU_m \rightarrow DT_n$ link and $DT_n \rightarrow DR_n$ link is required, which incurs an overhead size of $2MNB$ bits. Since only the CSI of the $DT_n \rightarrow DR_n$ link is required for the overlay mode,

the overhead size is MNB bits. Due to the need for the BS to perform mode selection, the CSI overhead size over the control channels for our system is $2MNB$ bits.

III. PROPOSED RESOURCE SCHEDULING SCHEME BASED ON ENERGY PRICE

Green communication, which aims to reduce EC and negative impacts on the environment without compromising users' QoS, is a trend that conveys sustainability for the communications industry. Efficient wireless scheduling allocation is an essential means to achieve green communication. For energy-constrained networks, prolonging the network lifetime is more critical than maximizing system throughput (Network lifetime may be defined in different ways depending on the application. This paper defines it as the time experienced from the initial status until any node in the network runs out of energy.). Because the latter will lead to rapid EC and frequent battery charging or replacement, contrary to the principle of green communication. Currently, the mainstream resource scheduling schemes for energy-constrained networks aim to maximize system EE or minimize system EC. However, these schemes may lead to unbalanced EC among different nodes, resulting in some nodes running out of energy more quickly.

To handle this problem, we design a resource scheduling scheme based on energy price in this section. At the beginning of each frame, the BS sets prices for the residual energy of CU_m and DT_n . Based on price theory [23], a node with more residual energy has a lower energy price, and vice versa. The EC among different nodes in the network will become more balanced through a reasonable pricing mechanism and a resource scheduling scheme according to minimum cost criteria. Thus, the network lifetime can be significantly extended.

In the remainder of this section, we first focus on the optimal power and spectrum allocation of cellular link m and D2D link n in the cooperative and overlay modes; then, we discuss the mode selection and link matching between M cell links and N D2D links; finally, we propose a heuristic pricing scheme which is suitable for real-time operation.

A. OPTIMAL POWER AND SPECTRUM ALLOCATION IN THE COOPERATIVE MODE

Denoting μ_m and μ_n as the energy prices of CU_m and DT_n , the cost paid by CU_m and DT_n within a frame can be expressed as $\mu_m\theta_{mn}p_{mb}T + \mu_n\theta_{mn}p_{nb}T$ and $\mu_n(1 - 2\theta_{mn})p_{nn}T$, respectively. Denote $C(m, n, i)$ as the total cost of cellular link m and D2D link n when the latter shares the channel of the former in mode i ($i = 1$ corresponds to the cooperative mode, $i = 2$ corresponds to the overlay mode). Therefore, we have

$$C(m, n, 1) = [\mu_m\theta_{mn}p_{mb} + \mu_n\theta_{mn}p_{nb} + \mu_n(1 - 2\theta_{mn})p_{nn}]T. \quad (5)$$

In order to extend the network lifetime, (5) needs to be minimized during each frame. The optimization problem can

be formulated as

$$\begin{aligned} \min_{p_{mb}, p_{nb}, p_{nn}, \theta_{mn}} \quad & \mu_m\theta_{mn}p_{mb} + \mu_n\theta_{mn}p_{nb} + \mu_n(1 - 2\theta_{mn})p_{nn}, \\ \text{s.t.} \quad & \begin{cases} p_{mb}\lambda_{mb} + p_{nb}\lambda_{nb} \geq 2Q_m/(W\theta_{mn}) - 1, \\ p_{mb} \geq p_{mb}^{low}, \\ p_{nn} \geq p_{nn}^{low}, \\ p_{mb}, p_{nb}, p_{nn} \leq P_{max}, \\ 0 < \theta_{mn} < 0.5, \end{cases} \end{aligned} \quad (6)$$

where the first three constraints correspond to the minimum rate requirement of cellular link m and D2D link n , which we denote as Q_m and Q_n , respectively. $p_{mb}^{low} = [2Q_m/(W\theta_{mn}) - 1]/\lambda_{mb}$, $p_{nn}^{low} = \{2Q_n/[W(1 - 2\theta_{mn})] - 1\}/\lambda_{nn}$ are the lower bound of p_{mb} and p_{nn} to make effective $CU_m \rightarrow DT_n$ link and $DT_n \rightarrow DR_n$ link guaranteeing the data transmission at the rate of Q_m and Q_n . Moreover, the fourth constraint corresponds to the limitations of the maximum transmit power of CU_m and DT_n . Without loss of generality, we assume they are equal and denoted by P_{max} .

Proposition 1: Problem (6) is nonconvex.

Proof: Denoting the objective function of problem (6) as $\Phi(p_{mb}, p_{nb}, p_{nn}, \theta_{mn})$, the Hessian matrix of Φ can be calculated as

$$\mathbf{H} = \begin{bmatrix} 0 & 0 & 0 & \mu_m \\ 0 & 0 & 0 & \mu_n \\ 0 & 0 & 0 & -2\mu_n \\ \mu_m & \mu_n & -2\mu_n & 0 \end{bmatrix}. \quad (7)$$

The characteristic polynomial of \mathbf{H} is given by

$$\det(\mathbf{H} - \lambda\mathbf{I}) = \lambda^2 \left(\lambda - \sqrt{\mu_m^2 + 5\mu_n^2} \right) \left(\lambda + \sqrt{\mu_m^2 + 5\mu_n^2} \right), \quad (8)$$

where \mathbf{I} is a 4×4 identity matrix.

By solving $\det(\mathbf{H} - \lambda\mathbf{I}) = 0$, we can get the eigenvalues of \mathbf{H} as $\lambda_1 = \lambda_2 = 0$, $\lambda_3 = \sqrt{\mu_m^2 + 5\mu_n^2} > 0$, $\lambda_4 = -\sqrt{\mu_m^2 + 5\mu_n^2} < 0$. Thus, \mathbf{H} is not positive semi-definite in the domain of problem (6). Therefore, Φ is not a convex function, and problem (6) is nonconvex [36].

In [29], the authors formulated a similar resource allocation problem in a cooperative cognitive radio network. Their optimization aimed to minimize the overall system EC, corresponding to the case that $\mu_m = \mu_n = 1$ in problem (6). However, they mistook the optimization problem for a convex problem and then directly applied Karush-Kuhn-Tucker (KKT) [36] conditions to obtain a unique global optimal solution, which does not exist. In this paper, to simplify problem (6), we divide it into two sub-problems. First, assuming that θ_{mn} is fixed, the power allocation problem can be transformed into a linear programming problem. Then, with the power allocation solution, we can obtain the spectrum allocation solution through Newton's method [36]. In section IV, we use simulation to prove that the power and spectrum allocation solution is optimal.

On the premise that θ_{mn} is fixed, it can be easily observed that Φ is a monotonically increasing function of p_{nn} .

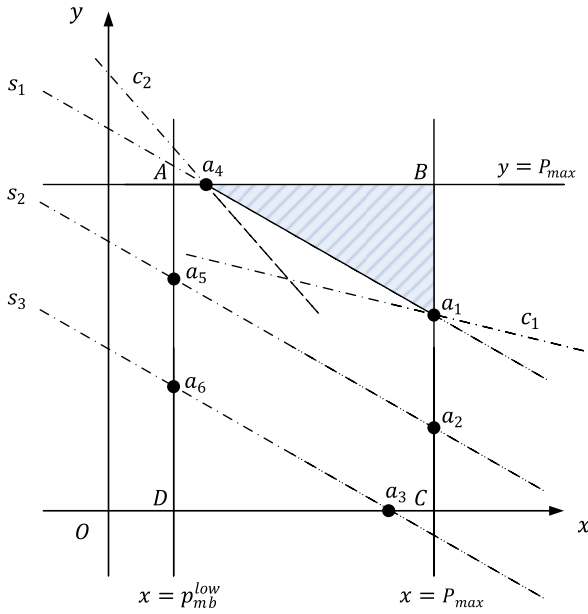


FIGURE 3. An illustration of the graphic method to find (p^*_mb, p^*_nb) .

Therefore, p_{nm} should take the minimum value in the domain of problem (6), i.e., $p^*_nm = p^{low}_{nm}$. How to find the optimal power allocation solution (p^*_mb, p^*_nb) is formulated as

$$\begin{aligned} \min_{p_{mb}, p_{nb}} \quad & \mu_m p_{mb} + \mu_n p_{nb}, \\ \text{s.t.} \quad & \begin{cases} p_{mb} \lambda_{mb} + p_{nb} \lambda_{nb} \geq 2Q_m / (W \theta_{mn}) - 1, \\ p^{low}_{mb} \leq p_{mb} \leq P_{max}, \\ 0 < p_{nb} \leq P_{max}. \end{cases} \end{aligned} \quad (9)$$

Problem (9) is a linear programming problem involving only two variables. By using x and y to represent p_{mb} and p_{nb} , it can be solved through the graphic method [37] in the xOy plane. For the sake of discussion, we define the following auxiliary functions

$$f(x, y) \triangleq \theta_{mn} W \log_2 (1 + \lambda_{mb} x + \lambda_{nb} y), \quad (10)$$

$$g(y) \triangleq \frac{1}{\lambda_{mb}} \left[2Q_m / (W \theta_{mn}) - 1 - \lambda_{nb} y \right], \quad (11)$$

$$h(x) \triangleq \frac{1}{\lambda_{nb}} \left[2Q_m / (W \theta_{mn}) - 1 - \lambda_{mb} x \right]. \quad (12)$$

We also denote k_c and k_s as the absolute values of the slope of isolines c : $\phi = \mu_m x + \mu_n y$ and s : $2Q_m / (W \theta_{mn}) - 1 = \lambda_{mb} x + \lambda_{nb} y$, where $k_c \triangleq \mu_m / \mu_n$, $k_s \triangleq \lambda_{mb} / \lambda_{nb}$, and ϕ is the objective function of problem (9). Denoting k_{AC} as the absolute value of the slope of straight line AC , we find that the relationship between k_s and k_{AC} is irrelevant to the solving process of problem (9). Thus, we take the case that $k_s < k_{AC}$ for example to illustrate the solving process, as shown in Fig. 3.

Isoline s divides the xOy plane into two half-planes. The intersection of the upper half-plane and the rectangle $ABCD$ represents the feasible region of problem (9), illustrated as the shaded region in Fig. 3. According to the different values of Q_m , there are three cases of s as follows.

- 1) s_1 corresponding to $f(p^{low}_{mb}, P_{max}) \leq Q_m \leq f(P_{max}, P_{max})$, denotes isoline s is below point $B(P_{max}, P_{max})$ (or passes through B) and above point $A(p^{low}_{mb}, P_{max})$ (or passes through A);
- 2) s_2 corresponding to $f(P_{max}, 0) < Q_m < f(p^{low}_{mb}, P_{max})$, denotes isoline s is below A and above point $C(P_{max}, 0)$;
- 3) s_3 corresponding to $f(p^{low}_{mb}, 0) < Q_m \leq f(P_{max}, 0)$, denotes isoline s is below C (or passes through C) and above point $D(p^{low}_{mb}, 0)$.

On the other hand, if isoline c moves up, ϕ will increase. Thus, the first intersection point of isoline c and the shaded region corresponds to (p^*_mb, p^*_nb) . When $Q_m > f(P_{max}, P_{max})$ or $p^{low}_{mb} > P_{max}$, the feasible region is \emptyset . When $Q_m \leq f(p^{low}_{mb}, 0)$ and $p^{low}_{mb} \leq P_{max}$, the feasible region is the entire rectangle $ABCD$ (when $p^{low}_{mb} = P_{max}$, the feasible region is the segment AD), and (p^*_mb, p^*_nb) lies on point $D(p^{low}_{mb}, 0)$. Since $p^*_nb = 0$, CU_m will not select DT_n as its relay in this situation. Therefore, the following derivation is based on the condition that $f(p^{low}_{mb}, 0) < Q_m \leq f(P_{max}, P_{max})$ and $p^{low}_{mb} \leq P_{max}$.

When $k_c < k_s$, isoline c corresponds to c_1 in Fig. 3, which indicates that the energy price of DT_n is relatively high. Thus, CU_m should purchase energy from DT_n as little as possible, and DT_n should utilize its energy as little as possible. Conversely, when $k_c \geq k_s$, isoline c corresponds to c_2 . CU_m should consume its energy as little as possible. Combining the value of Q_m , the optimal solution (p^*_mb, p^*_nb) can be obtained as follows.

Case 1: When $k_c < k_s$ and $f(P_{max}, 0) < Q_m \leq f(P_{max}, P_{max})$, the solution lies on the segment BC (except C), such as point a_1 or a_2 . We have $(p^*_mb, p^*_nb) = (P_{max}, h(P_{max}))$. The objective function of problem (6) can be rewritten as

$$\begin{aligned} \Phi(\theta_{mn}) = & \mu_m \theta_{mn} P_{max} \\ & + \frac{\mu_n \theta_{mn}}{\lambda_{nb}} \left[2Q_m / (W \theta_{mn}) - 1 - \lambda_{mb} P_{max} \right] \\ & + \frac{\mu_n (1 - 2\theta_{mn})}{\lambda_{nn}} \left\{ 2Q_n / [W(1 - 2\theta_{mn})] - 1 \right\}. \end{aligned} \quad (13)$$

The first and second derivatives of $\Phi(\theta_{mn})$ are represented as

$$\begin{aligned} \varphi(\theta_{mn}) = & \mu_m P_{max} + \frac{\mu_n}{\lambda_{nb}} \left[\left(1 - \frac{Q_m \ln 2}{W \theta_{mn}} \right) 2Q_m / (W \theta_{mn}) \right. \\ & \left. - 1 - \lambda_{mb} P_{max} \right] - \frac{2\mu_n}{\lambda_{nn}} \\ & \times \left\{ \left(1 - \frac{Q_n \ln 2}{W(1 - 2\theta_{mn})} \right) 2Q_n / [W(1 - 2\theta_{mn})] - 1 \right\}, \end{aligned} \quad (14)$$

$$\begin{aligned} \varphi'(\theta_{mn}) = & \frac{\mu_n}{\lambda_{nb}} \frac{(Q_m \ln 2)^2}{W^2 \theta_{mn}^3} 2Q_m / (W \theta_{mn}) \\ & + \frac{4\mu_n}{\lambda_{nn}} \frac{(Q_n \ln 2)^2}{W^2 (1 - 2\theta_{mn})^3} 2Q_n / [W(1 - 2\theta_{mn})]. \end{aligned} \quad (15)$$

TABLE 2. Four cases to obtain (p_{mb}^*, p_{nb}^*) .

Case	Relationship between k_s and k_c	Values range of Q_m	Solution	Corresponding point in Fig. 3
1	$k_c < k_s$	$f(P_{max}, 0) < Q_m \leq f(P_{max}, P_{max})$	$(P_{max}, h(P_{max}))$	a_1 or a_2
2	$k_c < k_s$	$f(p_{mb}^{low}, 0) < Q_m \leq f(P_{max}, 0)$	$(g(0), 0)$	a_3
3	$k_c \geq k_s$	$f(p_{mb}^{low}, P_{max}) \leq Q_m \leq f(P_{max}, P_{max})$	$(g(P_{max}), P_{max})$	a_4
4	$k_c \geq k_s$	$f(p_{mb}^{low}, 0) < Q_m < f(p_{mb}^{low}, P_{max})$	$(p_{mb}^{low}, h(p_{mb}^{low}))$	a_5 or a_6

Case 2: When $k_c < k_s$ and $f(p_{mb}^{low}, 0) < Q_m \leq f(P_{max}, 0)$, the solution lies on segment CD (except D), such as point a_3 . $(p_{mb}^*, p_{nb}^*) = (g(0), 0)$. Then we have

$$\Phi(\theta_{mn}) = \frac{\mu_m \theta_{mn}}{\lambda_{mb}} \left[2^{Q_m/(W\theta_{mn})} - 1 \right] + \frac{\mu_n (1 - 2\theta_{mn})}{\lambda_{nn}} \left\{ 2^{Q_n/[W(1-2\theta_{mn})]} - 1 \right\}, \quad (16)$$

$$\varphi(\theta_{mn}) = \frac{\mu_m}{\lambda_{mb}} \left[\left(1 - \frac{Q_m \ln 2}{W\theta_{mn}} \right) 2^{Q_m/(W\theta_{mn})} - 1 \right] - \frac{2\mu_n}{\lambda_{nn}} \times \left\{ \left(1 - \frac{Q_n \ln 2}{W(1-2\theta_{mn})} \right) 2^{Q_n/[W(1-2\theta_{mn})]} - 1 \right\}, \quad (17)$$

$$\varphi'(\theta_{mn}) = \frac{\mu_m (Q_m \ln 2)^2}{\lambda_{mb} W^2 \theta_{mn}^3} 2^{Q_m/(W\theta_{mn})} + \frac{4\mu_n (Q_n \ln 2)^2}{\lambda_{nn} W^2 (1 - 2\theta_{mn})^3} 2^{Q_n/[W(1-2\theta_{mn})]}. \quad (18)$$

Case 3: When $k_c \geq k_s$ and $f(p_{mb}^{low}, P_{max}) \leq Q_m \leq f(P_{max}, P_{max})$, the solution lies on segment AB, such as point a_4 . $(p_{mb}^*, p_{nb}^*) = (g(P_{max}), P_{max})$. There are

$$\Phi(\theta_{mn}) = \frac{\mu_m \theta_{mn}}{\lambda_{mb}} \left[2^{Q_m/(W\theta_{mn})} - 1 - \lambda_{nb} P_{max} \right] + \mu_n \theta_{mn} P_{max} + \frac{\mu_n (1 - 2\theta_{mn})}{\lambda_{nn}} \left\{ 2^{Q_n/[W(1-2\theta_{mn})]} - 1 \right\}, \quad (19)$$

$$\varphi(\theta_{mn}) = \frac{\mu_m}{\lambda_{mb}} \left[\left(1 - \frac{Q_m \ln 2}{W\theta_{mn}} \right) 2^{Q_m/(W\theta_{mn})} - 1 - \lambda_{nb} P_{max} \right] + \mu_n P_{max} - \frac{2\mu_n}{\lambda_{nn}} \left\{ \left(1 - \frac{Q_n \ln 2}{W(1-2\theta_{mn})} \right) 2^{Q_n/[W(1-2\theta_{mn})]} - 1 \right\}, \quad (20)$$

$$\varphi'(\theta_{mn}) = \frac{\mu_m (Q_m \ln 2)^2}{\lambda_{mb} W^2 \theta_{mn}^3} 2^{Q_m/(W\theta_{mn})} + \frac{4\mu_n (Q_n \ln 2)^2}{\lambda_{nn} W^2 (1 - 2\theta_{mn})^3} 2^{Q_n/[W(1-2\theta_{mn})]}. \quad (21)$$

Case 4: When $k_c \geq k_s$ and $f(p_{mb}^{low}, 0) < Q_m < f(p_{mb}^{low}, P_{max})$, the solution lies on segment AD (except

A and D), such as point a_5 or a_6 . $(p_{mb}^*, p_{nb}^*) = (p_{mb}^{low}, h(p_{mb}^{low}))$. There are

$$\Phi(\theta_{mn}) = \frac{\mu_n \theta_{mn}}{\lambda_{mn}} \left(\frac{\lambda_{mn}}{\lambda_{nb}} + k_c - k_s \right) \left[2^{Q_m/(W\theta_{mn})} - 1 \right] + \frac{\mu_n (1 - 2\theta_{mn})}{\lambda_{nn}} \left\{ 2^{Q_n/[W(1-2\theta_{mn})]} - 1 \right\}, \quad (22)$$

$$\varphi(\theta_{mn}) = \frac{\mu_n}{\lambda_{mn}} \left(\frac{\lambda_{mn}}{\lambda_{nb}} + k_c - k_s \right) \left[\left(1 - \frac{Q_m \ln 2}{W\theta_{mn}} \right) 2^{Q_m/(W\theta_{mn})} - 1 \right] - \frac{2\mu_n}{\lambda_{nn}} \left\{ \left(1 - \frac{Q_n \ln 2}{W(1-2\theta_{mn})} \right) 2^{Q_n/[W(1-2\theta_{mn})]} - 1 \right\}, \quad (23)$$

$$\varphi'(\theta_{mn}) = \frac{\mu_n}{\lambda_{mn}} \left(\frac{\lambda_{mn}}{\lambda_{nb}} + k_c - k_s \right) \frac{(Q_m \ln 2)^2}{W^2 \theta_{mn}^3} 2^{Q_m/(W\theta_{mn})} + \frac{4\mu_n (Q_n \ln 2)^2}{\lambda_{nn} W^2 (1 - 2\theta_{mn})^3} 2^{Q_n/[W(1-2\theta_{mn})]}. \quad (24)$$

For all the four cases above, since $\theta_{mn} \in (0, 0.5)$, the inequality $\varphi'(\theta_{mn}) > 0$ holds. $\varphi(\theta_{mn})$ is monotonically increasing. Note that

$$\lim_{\theta_{mn} \rightarrow 0^+} \varphi(\theta_{mn}) = -\infty \text{ and } \lim_{\theta_{mn} \rightarrow 0.5^-} \varphi(\theta_{mn}) = +\infty.$$

Hence, there exists a θ'_{mn} which satisfies $\varphi(\theta'_{mn}) = 0$. When $\theta_{mn} \in (0, \theta'_{mn})$, $\varphi(\theta_{mn}) < 0$ holds. $\Phi(\theta_{mn})$ is monotonically decreasing. When $\theta_{mn} \in (\theta'_{mn}, 0.5)$, $\varphi(\theta_{mn}) > 0$ holds. $\Phi(\theta_{mn})$ is monotonically increasing. So $\Phi(\theta_{mn})$ achieves a unique minimum at θ'_{mn} , i.e., $\theta_{mn}^* = \theta'_{mn}$.

In this paper, we use Newton's method to find the optimal spectrum allocation strategy θ_{mn}^* as follows.

1) Take $\theta_{mn}^{(1)} \in (0, 0.5)$ as the initial value of the iterative algorithm.

2) Denoting $\theta_{mn}^{(k)}$ as an approximate value of θ_{mn}^* after the k -th iteration, an even better $\theta_{mn}^{(k+1)}$ is given by

$$\theta_{mn}^{(k+1)} = \theta_{mn}^{(k)} - \frac{\varphi(\theta_{mn}^{(k)})}{\varphi'(\theta_{mn}^{(k)})}. \quad (25)$$

3) If the termination criterion $|\theta_{mn}^{(k+1)} - \theta_{mn}^{(k)}| \leq \varepsilon_0$ satisfies, we have $\theta_{mn}^* \approx \theta_{mn}^{(k+1)}$, where ε_0 is a positive number that is small enough.

It is worth noting that the computational process to achieve $(p_{mb}^*, p_{nb}^*, p_{nn}^*, \theta_{mn}^*)$ is opposite to the above analysis process. The optimal power allocation can be obtained only by using Newton's method to get θ_{mn}^* first. Moreover, if θ_{mn}^* is obtained in case 2, we have $p_{nb}^* = 0$. The cooperative communication between CU_m and DT_n will not be implemented.

B. OPTIMAL POWER AND SPECTRUM ALLOCATION IN THE OVERLAY MODE

In the overlay mode, the cost paid by CU_m and DT_n within a frame when D2D link n shares the channel of cellular link m is given by

$$C(m, n, 2) = [\mu_m \alpha_{mn} p_{mb} + \mu_n (1 - \alpha_{mn}) p_{nn}] T. \quad (26)$$

The optimal power and spectrum allocation problem, according to the minimum cost criterion, is formulated as

$$\begin{aligned} \min_{p_{mb}, p_{nn}, \alpha_{mn}} & \mu_m \alpha_{mn} p_{mb} + \mu_n (1 - \alpha_{mn}) p_{nn}, \\ \text{s.t.} & \begin{cases} p_{mb} \geq [2Q_m / (W \alpha_{mn}) - 1] / \lambda_{mb}, \\ p_{nn} \geq \{2Q_n / [W(1 - \alpha_{mn})] - 1\} / \lambda_{nn}, \\ p_{mb}, p_{nn} \leq P_{max}, \\ 0 < \alpha_{mn} < 1, \end{cases} \end{aligned} \quad (27)$$

where the first and second constraints correspond to the minimum rate requirement Q_m and Q_n , respectively. The third constraint corresponds to the limitations of the maximum transmit power of CU_m and DT_n .

We denote the objective function of problem (27) as $\Psi(p_{mb}, p_{nn}, \alpha_{mn})$. Noting that Ψ is a monotonically increasing function of p_{mb} and p_{nn} , when α_{mn} is fixed, we have $p_{mb}^* = [2Q_m / (W \alpha_{mn}) - 1] / \lambda_{mb}$ and $p_{nn}^* = \{2Q_n / [W(1 - \alpha_{mn})] - 1\} / \lambda_{nn}$. Thus, substituting p_{mb}^* and p_{nn}^* into Ψ , it can be rewritten as

$$\begin{aligned} \Psi(\alpha_{mn}) &= \mu_m \alpha_{mn} [2Q_m / (W \alpha_{mn}) - 1] / \lambda_{mb} + \mu_n (1 - \alpha_{mn}) \\ &\quad \times \{2Q_n / [W(1 - \alpha_{mn})] - 1\} / \lambda_{nn}. \end{aligned} \quad (28)$$

The first and second derivatives of $\Psi(\alpha_{mn})$ are represented as

$$\begin{aligned} \psi(\alpha_{mn}) &= \frac{\mu_m}{\lambda_{mb}} \left[\left(1 - \frac{Q_m \ln 2}{W \alpha_{mn}} \right) 2Q_m / (W \alpha_{mn}) - 1 \right] \\ &\quad - \frac{\mu_n}{\lambda_{nn}} \left\{ \left(1 - \frac{Q_n \ln 2}{W(1 - \alpha_{mn})} \right) 2Q_n / [W(1 - \alpha_{mn})] - 1 \right\}, \end{aligned} \quad (29)$$

$$\begin{aligned} \psi'(\alpha_{mn}) &= \frac{\mu_m}{\lambda_{mb}} \frac{(Q_m \ln 2)^2}{W^2 \alpha_{mn}^3} 2Q_m / (W \alpha_{mn}) \\ &\quad + \frac{\mu_n}{\lambda_{nn}} \frac{(Q_n \ln 2)^2}{W^2 (1 - \alpha_{mn})^3} 2Q_n / [W(1 - \alpha_{mn})]. \end{aligned} \quad (30)$$

Since $\alpha_{mn} \in (0, 1)$, we obtain inequality $\psi'(\alpha_{mn}) > 0$. On the other hand, it is easy to verify that

$$\lim_{\alpha_{mn} \rightarrow 0^+} \psi(\alpha_{mn}) = -\infty \text{ and } \lim_{\alpha_{mn} \rightarrow 1^-} \psi(\alpha_{mn}) = +\infty.$$

Consequently, using Newton's method, we can obtain the optimal spectrum allocation strategy α_{mn}^* similarly as described before.

Cellular links

D2D links

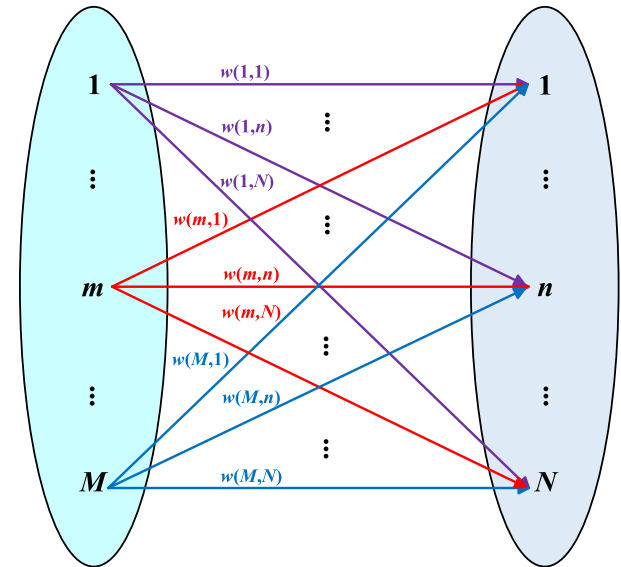


FIGURE 4. The weighted bipartite graph corresponding to the mode selection and link matching problem.

C. MODE SELECTION AND LINK MATCHING

In our proposed communication framework, the BS schedules resources between the cellular and D2D links according to the QoS requirements, energy prices, and collected CSI. With $\{C(m, n, i) | m \in \mathcal{M}, n \in \mathcal{N}, i = 1 \text{ or } 2\}$ obtained above, the mode selection and link matching strategy π , which aims to minimize the overall system cost, is formulated as a weighted bipartite matching problem. We can construct the corresponding bipartite graph as Fig. 4 with the weight

$$w(m, n) = V - v(m, n), \quad (31)$$

where $v(m, n) = \min\{C(m, n, 1), C(m, n, 2)\}$, and V is a constant which satisfies $V \geq \max\{v(1, 1), \dots, v(M, N)\}$.

If Q_n cannot be guaranteed in either the cooperative mode or overlay mode, D2D link n will not share the channel of cellular link m . The optimal transmit power of CU_m is $p_{mb}^* = (2Q_m / W - 1) / \lambda_{mb}$ during the entire frame, and we set $C(m, n, 1) = C(m, n, 2) = V$. Through the Kuhn-Munkres algorithm [38], the optimal mode selection and link matching strategy π^* between \mathcal{M} and \mathcal{N} can be determined with the time complexity of $O(\max\{M, N\}^3)$.

D. ENERGY PRICING STRATEGY

The energy prices will significantly affect the EC of each node in our system. The energy price of a node implies its own willingness or that of its corresponding nodes to consume or buy its energy. Thus, it is essential to establish a reasonable energy pricing strategy. How to set the optimal prices has been extensively investigated under mathematical frameworks such as game theory [8], [9] and general equilibrium theory [39]. Most existing works started with designing utility functions. One user's utility function

comprises gain and loss, usually measured through two performance metrics. For instance, if we refer to the problem formulation section in [26], the gain of D2D link m in the cooperative mode is its achievable rate given by (2), and the loss is its average power consumption given by $(1 - 2\theta_{mm})p_{mm}$. The price μ_n links them. In order to set the price, we need to design a utility function carefully [27]. Moreover, there is also a need to introduce extra auxiliary parameters and make some assumptions or simplifications [25], [26], which differ from actual economic activities and may lack convincingness.

On the other hand, most pricing methods in these works are based on iterative algorithms, which will introduce massive communication and computation overheads. Take general equilibrium theory as an example. The equilibrium price is the only price where the supply and demand are balanced. Achieving this price needs information sharing and bargaining between each node in our system, which hinders real-time operation [40].

In order to reduce communication overhead and make our algorithm more efficient, we attempt to utilize a heuristic pricing strategy that involves no iteration and supposes the energy prices of CU_m and DT_n during the t -th frame are inversely proportional to their residual energy as follows.

$$\mu_m^{(t)} = \mu_m^{(1)} \frac{E_m^{(1)}}{E_m^{(t)}}, \quad (32)$$

$$\mu_n^{(t)} = \mu_n^{(1)} \frac{E_n^{(1)}}{E_n^{(t)}}, \quad (33)$$

where $\mu_m^{(1)}$ and $\mu_n^{(1)}$ denote the initial energy prices of CU_m and DT_n . $E_m^{(1)}$ and $E_n^{(1)}$ denote the initial battery energy of CU_m and DT_n . Moreover, $E_m^{(t)}$ and $E_n^{(t)}$ represent the residual battery energy of CU_m and DT_n at the beginning of the t -th frame, respectively.

Remark 3: To update the energy prices of CU_m and DT_n , the value of their residual energy must be sent to the BS through control channels at the beginning of each frame. Thus, the size of the energy state information overhead over the control channels for our proposed communication framework is $2MND$ bits, where D indicates the size of an energy state information report. If we make the energy prices equal for all the nodes during each frame, the BS needs no energy state information. In this case, problem (6) minimizes the overall system EC.

IV. SIMULATION RESULTS

In this section, the performance of our proposed resource scheduling scheme based on energy price is validated through simulations. The channel gains are given by a simplified path loss model $h = \xi d^{-\gamma}$, where ξ is the multipath fading gain with a Rayleigh distribution, d is the distance between a transmitter and a receiver, and γ is the path loss exponent. Unless otherwise specified, simulation parameters are set as shown in Table 3. We employ the Monte Carlo simulation and

obtain all the results based on 1000 simulation runs without a specific illustration.

Algorithm: The resource scheduling scheme based on energy price

```

1: Set  $t = 1$ ;
2: while  $E_m^{(t)} > 0, \forall m \in \mathcal{M}$  and  $E_n^{(t)} > 0, \forall n \in \mathcal{N}$  do
3:   for each  $m \in \mathcal{M}$  do
4:     for each  $n \in \mathcal{N}$  do
5:       Calculate  $\theta_{mn}^*$  and  $\alpha_{mn}^*$  through Newton's method;
6:       Calculate  $(p_{mb}^*, p_{nb}^*, p_{nn}^*)$  and  $(p_{mb}^*, p_{nn}^*)$  for the
         cooperative and overlay modes;
7:       for  $i \in \{1, 2\}$  do
8:         if  $R_n \geq Q_n$  in mode  $i$  then
9:           Calculate  $C(m, n, i)$ ;
10:        else
11:          Set  $C(m, n, i) = V$ ;
12:        end if
13:      end for
14:    end for
15:  end for
16:  Obtain  $\pi^*$  through the Kuhn-Munkres algorithm;
17:  for each  $m \in \mathcal{M}$  do
18:    for each  $n \in \mathcal{N}$  do
19:      Calculate  $E_m^{(t+1)}$  and  $E_n^{(t+1)}$ ;
20:      Update  $\mu_m^{(t+1)}$  and  $\mu_n^{(t+1)}$  according to (31) and (32);
21:    end for
22:  end for
23:   $t \leftarrow t + 1$ ;
24: end while

```

TABLE 3. Simulation parameters.

Simulation parameter	Value
Cell radius (R)	1000 m (for part B)
Path loss exponent (γ)	3.8
Channel bandwidth (W)	10 kHz
Frame length (T)	1 ms
Gaussian noise spectral density (n_0)	-174 dBm/Hz
Maximum transmit power (P_{max})	23 dBm
Distance between CU_m and the BS (d_{mb})	1000 m (for part A)
Distance between DT_n and the BS (d_{nb})	500 m (for part A)
Initial battery energy of CU_m ($E_m^{(1)}$)	1 mJ
Initial battery energy of DT_n ($E_n^{(1)}$)	1 mJ
Initial energy prices of CU_m ($\mu_m^{(1)}$)	1
Initial energy prices of DT_n ($\mu_n^{(1)}$)	1
Number of cellular links (M)	5 (for part B)
Number of D2D links (N)	1~10 (for part B)
Minimum rate requirement of cellular link $m \in \mathcal{M}$ (Q_m)	10 kbps
Minimum rate requirement of D2D link $n \in \mathcal{N}$ (Q_n)	5 kbps
Iteration termination parameter (ϵ_0)	10^{-6}

A. PERFORMANCE OF CELLULAR LINK m AND D2D LINK n

First, we investigate the performance of the proposed scheme when D2D link n shares the channel of cellular link m within the first frame. In this subsection, we set the distance between CU_m and the BS as $d_{mb} = 1000$ m, and the distance between DT_n and the BS as $d_{nb} = 500$ m, respectively. d_{mn} denotes the distance between CU_m and DT_n . d_{nn} denotes the distance between DT_n and DR_n .

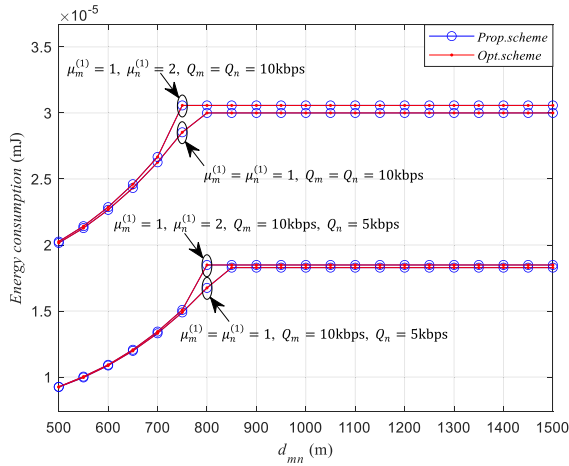


FIGURE 5. The total EC of cellular link m and D2D link n versus d_{mn} for different initial energy prices and minimum rate requirements to verify the optimality of the proposed scheme.

To verify the optimality of the proposed power and spectrum allocation scheme, we compare it with the optimal scheme implemented through an exhaustive search. Fig. 5 shows the total EC of cellular link m and D2D link n as a function of d_{mn} when $d_{nn} = 1000$ m. Since the triangle inequality $|d_{mb} - d_{nb}| \leq d_{mn} \leq d_{mb} + d_{nb}$ should be satisfied, we set $500 \text{ m} \leq d_{mn} \leq 1500$ m. It can be observed that the curves of the two schemes overlap for different initial energy prices and minimum rate requirements, which means that the two schemes have the same performance. The same phenomenon occurs under other simulation parameter configurations, which implies that the proposed scheme is optimal.

Next, we set $\mu_m^{(1)} = \mu_n^{(1)} = 1$, $Q_m = 10$ kbps and $Q_n = 5$ kbps. In this situation, the proposed scheme is equivalent to the minimum EC scheme. We compare the proposed scheme with the proposed scheme with fixed spectrum allocation ($\alpha_{mn} = 1/2$, $\theta_{mn} = 1/4$) and the maximum EE scheme. In particular, the optimal power and spectrum allocation is identified through an exhaustive search in the maximum EE scheme. In Fig. 6, we show the achievable rates of cellular link m and D2D link n versus d_{mn} when $d_{nn} = 1000$ m. It can be observed that the considered schemes can guarantee the minimum rate requirements of these two links, which are equal to their achievable rates, i.e., $R_m = Q_m$ and $R_n = Q_n$. This result indicates that we can evaluate their performance in terms of EE through EC.

Remark 4: The resource allocation problem to maximize the EE of our system can be formulated by replacing the objective functions of problems (6) and (27). For example, in the cooperative mode, the EE of our system can be denoted as follows, as shown in the equation (34) at the bottom of this page.

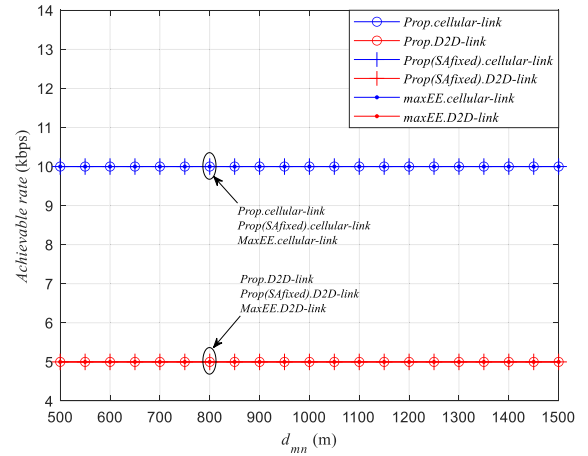


FIGURE 6. The achievable rates of cellular link m and D2D link n versus d_{mn} .

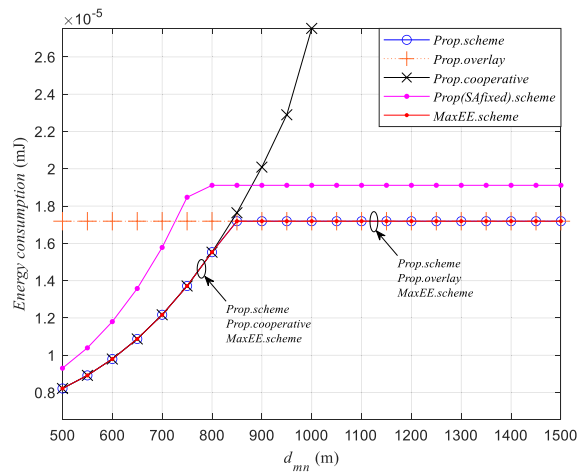


FIGURE 7. The total EC of cellular link m and D2D link n versus d_{mn} .

It is a nonconvex function, so its corresponding optimal problem is nonconvex and hard to tackle. To the best of our knowledge, existing studies have yet to give a solution to this problem. Thus, our simulation identifies the maximum EE scheme through an exhaustive search.

The computational complexity of the proposed resource scheduling scheme, the proposed scheme with fixed spectrum allocation, and the maximum EE scheme within one frame is $O(\max\{M, N\}^3 + 2MNU)$, $O(\max\{M, N\}^3 + 2MN)$ and $O(\max\{M, N\}^3 + 2MNV)$, respectively, where U and V denote the time granularities of Newton's method and the exhaustive search.

Fig. 7 presents the total EC of cellular link m and D2D link n versus d_{mn} when $d_{nn} = 950$ m. In addition to the three schemes above, we consider the proposed scheme in the cooperative mode and the proposed scheme in the overlay mode. Since problem (27) is irrelevant to d_{mn} , the performance of the proposed scheme in the overlay mode is

$$\eta = \frac{\theta_{mn} W \log_2(1 + \min\{p_{mb}\lambda_{mn}, p_{mb}\lambda_{mb} + p_{nb}\lambda_{nb}\}) + (1 - 2\theta_{mn}) W \log_2(1 + p_{nn}\lambda_{nn})}{\theta_{mn} p_{mb} + \theta_{nn} p_{nb} + (1 - 2\theta_{mn}) p_{nn}} \quad (34)$$

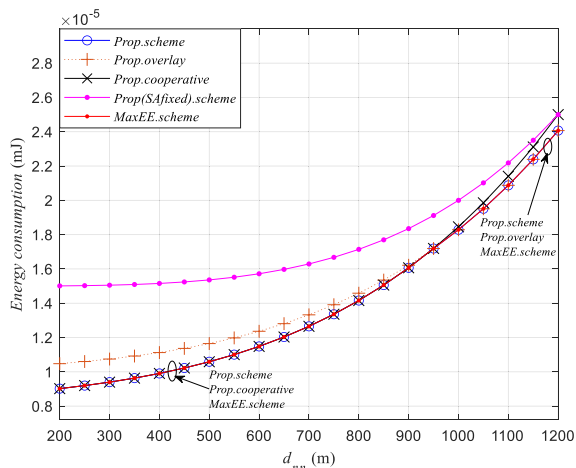


FIGURE 8. The total EC of cellular link m and D2D link n versus d_{mn} .

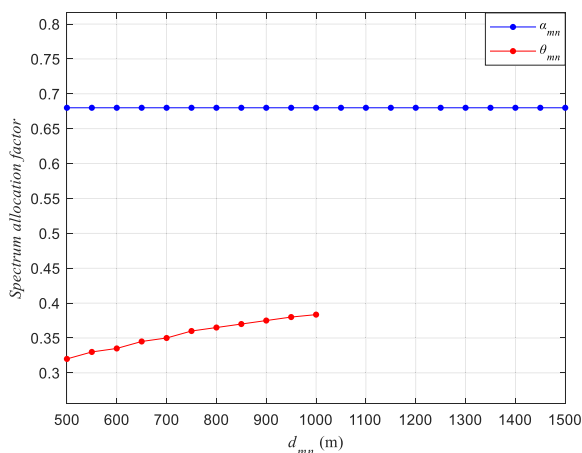


FIGURE 9. The spectrum allocation factor of the proposed scheme versus d_{mn} .

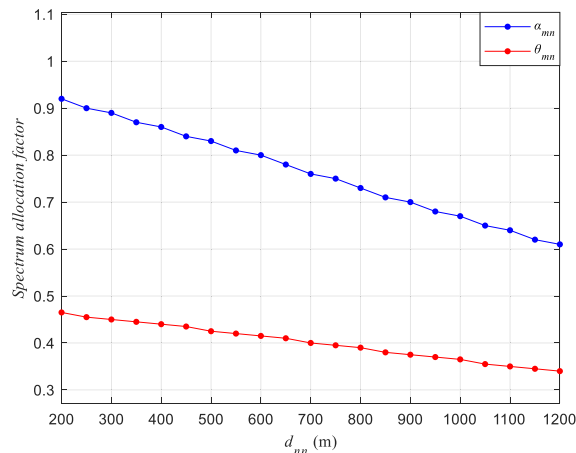


FIGURE 10. The spectrum allocation factor of the proposed scheme versus d_{mn} .

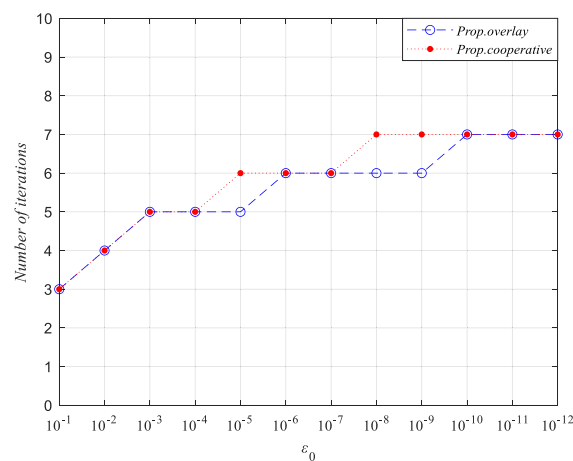


FIGURE 11. The number of iterations versus ϵ_0 .

invariable. We can observe that the proposed scheme switches from the cooperative mode to the overlay mode at $d_{mn} = 840$ m, and has the lowest EC. It is worth noting that the EC of the proposed scheme in the cooperative mode takes no value when $d_{mn} > 1000$ m, which implies that the minimum rate requirement of cellular link m cannot be guaranteed. This figure also shows that the proposed scheme has the same performance as the maximum EE scheme, and its EC is reduced by about 13% compared with the proposed scheme with fixed spectrum allocation. Combining the results shown in Fig. 6, we conclude that the EE of the proposed scheme is also optimal in this scenario. However, its complexity is much lower than that of the maximum EE scheme.

Fig. 8 shows the total EC versus d_{mn} when $d_{mn} = 840$ m. The proposed scheme switches from the cooperative mode to the overlay mode at $d_{mn} = 950$ m. Similar to Fig. 7, it is clear that the proposed scheme has the same performance as the maximum EE scheme and outperforms the proposed scheme with fixed spectrum allocation. For instance, when d_{mn} is increased from 200 m to 500 m, the EC of the proposed scheme is reduced by more than 30% compared with the proposed scheme with fixed spectrum allocation.

Fig. 9 shows the spectrum allocation factor of the proposed scheme as a function of d_{mn} when $d_{mn} = 950$ m. For the same reason explained in Fig. 7, α_{mn} is a constant, and when $d_{mn} > 1000$ m, θ_{mn} takes no value. We can observe that θ_{mn} increases as d_{mn} increases from 500 m to 1000 m. The explanation is as follows. When d_{mn} increases, the channel gain of the $CU_m \rightarrow DT_n$ link decreases. To guarantee the QoS of CU_m and minimize the total EC, the BS should allocate more spectrum to CU_m in the time domain. Similar to Fig. 9, Fig. 10 shows the spectrum allocation factor of the proposed scheme versus d_{mn} when $d_{mn} = 840$ m.

In Fig. 11, we show the number of iterations to achieve the optimal spectrum allocation factors through Newton's method in the cooperative and overlay modes against ϵ_0 when $d_{mn} = 840$ m and $d_{mn} = 950$ m. We can observe from the simulation results that it takes five iterations for the proposed scheme to converge when $\epsilon_0 = 10^{-4}$. Even if $\epsilon_0 = 10^{-12}$, it only requires two more iterations to converge, which indicates the proposed joint power and spectrum allocation scheme is suitable for real-time operations.

In Fig. 12, we present the EC versus price ratio $\mu_n^{(1)} / \mu_m^{(1)}$ in the first frame when $d_{mn} = 840$ m and $d_{mn} = 950$ m.

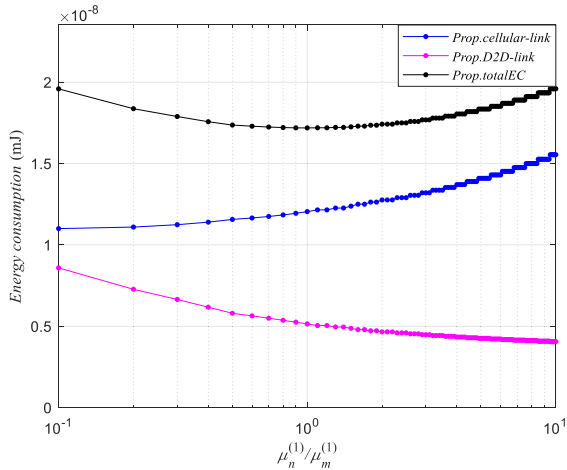


FIGURE 12. The EC versus $\mu_n^{(1)}/\mu_m^{(1)}$.

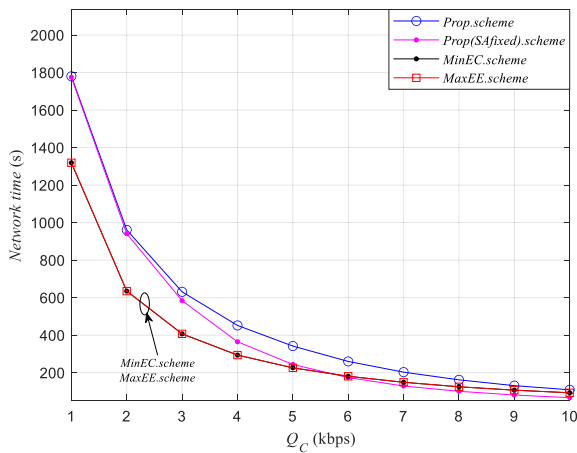


FIGURE 13. The network lifetime of cellular link m and D2D link n versus Q_m .

On the one hand, with the increasing $\mu_n^{(1)}/\mu_m^{(1)}$, the EC of cellular link m increases and that of D2D link n decreases. This phenomenon implies that CU_m will purchase energy from DT_n as little as possible and utilize the energy itself as much as possible to guarantee its minimum rate requirement when the energy price of DT_n is relatively higher than that of CU_m . For the same reason, DT_n will consume as little energy as possible if its minimum rate requirement is guaranteed. On the other hand, if $\mu_n^{(1)}/\mu_m^{(1)}$ is too low or too high, the total EC of cellular link m and D2D link n will increase. Then, D2D link n will attempt to match with another cellular link. As a result, with the price inversely proportional to the residual energy of each node, the overall system EC will be controlled at a low level, and each node's EC will be balanced in the final matching.

Fig. 13 investigates the performance of the proposed schemes in terms of network lifetime for varying Q_m . We compare the proposed scheme with the proposed scheme with fixed spectrum allocation, the maximum EE scheme, and the minimum EC scheme. The latter corresponds to the proposed scheme with $\mu_m^{(t)} = \mu_n^{(t)} = 1$. We set $d_{mm} = 800$ m, $d_{nn} = 500$ m, $Q_n = 5$ kbps and $\mu_m^{(1)} = \mu_n^{(1)} = 1$.

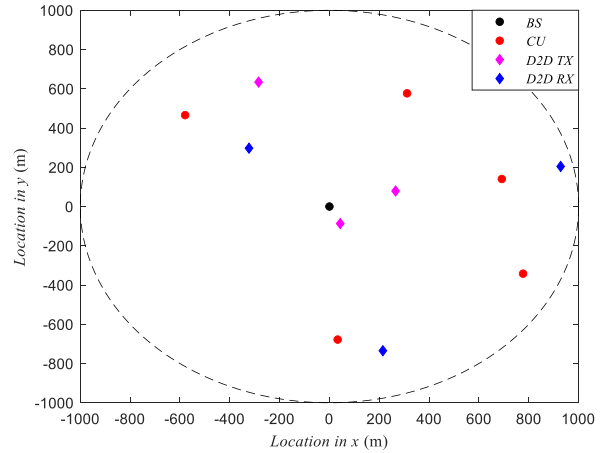


FIGURE 14. A snapshot of user locations for a single cellular network with M cellular and N D2D links ($M = 5$ and $N = 3$).

Since a larger Q_m leads to higher EC, the network lifetime of all the considered schemes decreases as Q_m increases. It can be observed that the minimum EC scheme has the same performance as the maximum EE scheme. However, the computational complexity of the latter is much greater than that of the former. The simulation results also show that the proposed scheme outperforms these two by about 40%, revealing its superiority. Moreover, the proposed scheme with fixed spectrum allocation has nearly the same performance as the proposed scheme when $1 \text{ kbps} \leq Q_m \leq 2 \text{ kbps}$, which indicates the importance of reasonable spectrum allocation.

B. PERFORMANCE OF M CELLULAR LINKS AND N D2D LINKS

In this part, we evaluate the performance of M cellular and N D2D links. In our simulations, the BS is deployed in the cell center with a radius $R = 1000$ m. The CUs and the D2D pairs are uniformly distributed within the cell. The minimum rate requirements of the cellular and D2D links are set to be 10 kbps and 5 kbps. Each node's initial energy price and battery energy are set to be 1 and 1 mJ, respectively. Fig. 14 shows a snapshot of user locations with $M = 5$ and $N = 3$. Fig. 15 shows the influence of changing N to the system throughput when $M = 5$. It is noted that the system throughput of the considered schemes is equal to $MQ_m + \min\{N, M\}Q_n$, which is consistent with the results in Fig. 6. The simulation results also imply that the number of the active D2D links is equal to 5 when $N > 5$.

Fig. 16 shows the impact of N on the network lifetime of the system. The results further confirm the superiority of the proposed scheme. Besides, it can be observed that the network lifetime decreases when $N \leq 5$ and increases slightly when $N > 5$ with the increasing N . The rationale is as follows. When $N \leq 5$, more active links consume energy as N increases, which shortens the time for any node in the system to exhaust its energy. When $N > 5$, the number of D2D links that access the channels of the cellular links is always equal to 5, which means that the number of active links no longer increases as N increases. On the other hand, the

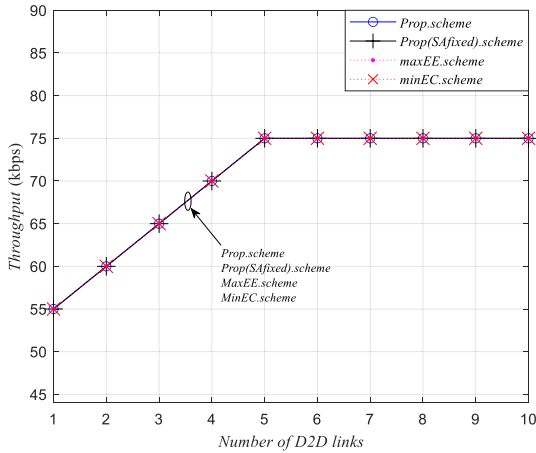


FIGURE 15. The system throughput versus N .

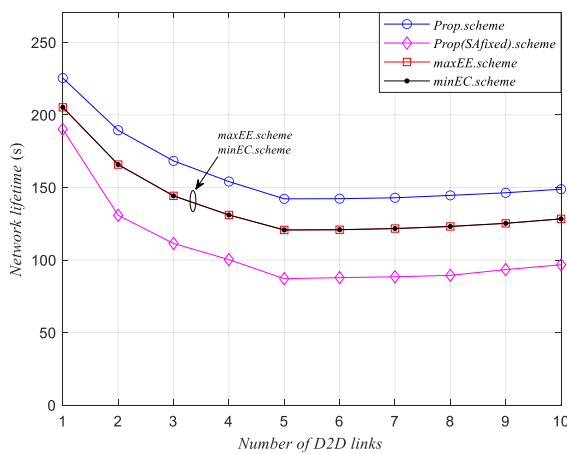


FIGURE 16. The network lifetime of the system versus N .

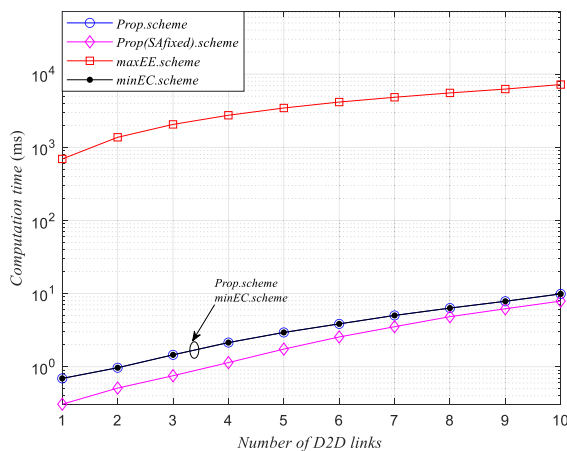


FIGURE 17. Computation time versus N .

potential matching between the cellular and D2D links still increases. Consequently, it will make the EC among different nodes more balanced, prolonging the network lifetime of the system.

Finally, Fig. 17 shows the average computation time versus N in the first frame. This simulation measures the computation time through an Intel Core i7-9750H with 16 GB

memory based on Matlab R2022b. It can be observed that the average computation time of the proposed scheme, the proposed scheme with fixed spectrum allocation, and the minimum EC scheme is kept low, while that of the maximum EE scheme is significantly increased, e.g., the computation time of the maximum EE scheme is more than 7000 ms when $N = 10$. The computation time of the proposed scheme equals that of the minimum EC scheme. We also notice that the computation time of the proposed scheme is higher than it is for the proposed scheme with fixed spectrum allocation, which does not involve Newton’s method. However, the computation time of the proposed scheme is always less than 10 ms for all the cases considered, which proves its suitability for real-time operation.

V. CONCLUSION

In this paper, we have investigated the resource scheduling issue in cooperative D2D communications overlaying cellular networks and proposed a scheme to jointly optimize power and spectrum allocation, mode selection, and link matching. Based on energy price, the utilization of each node’s energy could be balanced, extending the network lifetime of our system. Through the graphic method and Newton’s method, an algorithm with low computational complexity was used to tackle the nonconvex power and spectrum allocation problem. Alongside the proposed scheme, we proposed a heuristic energy pricing strategy that involved no iteration and was suitable for real-time operation. The simulations demonstrated the advantage of the proposed scheme. When the energy prices of different nodes are equal, the optimality of the proposed scheme in terms of EE was also verified in our scenario.

REFERENCES

- [1] A. Damjanovic, J. Montojo, Y. Wei, T. Ji, T. Luo, M. Vajapeyam, T. Yoo, O. Song, and D. Malladi, “A survey on 3GPP heterogeneous networks,” *IEEE Wireless Commun.*, vol. 18, no. 3, pp. 10–21, Jun. 2011, doi: 10.1109/MWC.2011.5876496.
- [2] L. Lu, G. Y. Li, A. L. Swindlehurst, A. Ashikhmin, and R. Zhang, “An overview of massive MIMO: Benefits and challenges,” *IEEE J. Sel. Topics Signal Process.*, vol. 8, no. 5, pp. 742–758, Oct. 2014, doi: 10.1109/JSTSP.2014.2317671.
- [3] A. Asadi, Q. Wang, and V. Mancuso, “A survey on device-to-device communication in cellular networks,” *IEEE Commun. Surveys Tuts.*, vol. 16, no. 4, pp. 1801–1819, 4th Quart., 2014, doi: 10.1109/COMST.2014.2319555.
- [4] R. Vannithamby and S. Talwar, “Device-to-device communications,” in *Towards 5G: Applications, Requirements and Candidate Technologies*. Hoboken, NJ, USA: Wiley, 2017, p. 162.
- [5] D. Feng, L. Lu, Y. Yuan-Wu, G. Y. Li, S. Li, and G. Feng, “Device-to-device communications in cellular networks,” *IEEE Commun. Mag.*, vol. 52, no. 4, pp. 49–55, Apr. 2014, doi: 10.1109/MCOM.2014.6807946.
- [6] J. N. Laneman, D. N. C. Tse, and G. W. Wornell, “Cooperative diversity in wireless networks: Efficient protocols and outage behavior,” *IEEE Trans. Inf. Theory*, vol. 50, no. 12, pp. 3062–3080, Dec. 2004, doi: 10.1109/TIT.2004.838089.
- [7] Y. Cao, T. Jiang, and C. Wang, “Cooperative device-to-device communications in cellular networks,” *IEEE Wireless Commun.*, vol. 22, no. 3, pp. 124–129, Jun. 2015, doi: 10.1109/MWC.2015.7143335.
- [8] Y. Yuan, T. Yang, H. Feng, and B. Hu, “Learning for matching game in cooperative D2D communication with incomplete information,” *IEEE Trans. Veh. Technol.*, vol. 68, no. 7, pp. 7174–7178, Jul. 2019, doi: 10.1109/TVT.2019.2914032.

- [9] Y. Yuan, T. Yang, Y. Hu, H. Feng, and B. Hu, "Two-timescale resource allocation for cooperative D2D communication: A matching game approach," *IEEE Trans. Veh. Technol.*, vol. 70, no. 1, pp. 543–557, Jan. 2021, doi: [10.1109/TVT.2020.3046747](https://doi.org/10.1109/TVT.2020.3046747).
- [10] J. Lee and J. H. Lee, "Performance analysis and resource allocation for cooperative D2D communication in cellular networks with multiple D2D pairs," *IEEE Commun. Lett.*, vol. 23, no. 5, pp. 909–912, May 2019, doi: [10.1109/LCOMM.2019.2907252](https://doi.org/10.1109/LCOMM.2019.2907252).
- [11] C. Ma, Y. Li, H. Yu, X. Gan, X. Wang, Y. Ren, and J. J. Xu, "Cooperative spectrum sharing in D2D-enabled cellular networks," *IEEE Trans. Commun.*, vol. 64, no. 10, pp. 4394–4408, Oct. 2016, doi: [10.1109/TCOMM.2016.2600674](https://doi.org/10.1109/TCOMM.2016.2600674).
- [12] S. Yu, W. U. Khan, X. Zhang, and J. Liu, "Optimal power allocation for NOMA-enabled D2D communication with imperfect SIC decoding," *Phys. Commun.*, vol. 46, Jun. 2021, Art. no. 101296, doi: [10.1016/J.PHYCOM.2021.101296](https://doi.org/10.1016/J.PHYCOM.2021.101296).
- [13] Y. Gao, Y. Xiao, M. Wu, M. Xiao, and J. Shao, "Dynamic social-aware peer selection for cooperative relay management with D2D communications," *IEEE Trans. Commun.*, vol. 67, no. 5, pp. 3124–3139, May 2019, doi: [10.1109/TCOMM.2019.2894138](https://doi.org/10.1109/TCOMM.2019.2894138).
- [14] D. Feng, C. Jiang, G. Lim, L. J. Cimini, G. Feng, and G. Y. Li, "A survey of energy-efficient wireless communications," *IEEE Commun. Surveys Tuts.*, vol. 15, no. 1, pp. 167–178, 1st Quart., 2013, doi: [10.1109/SURV.2012.020212.00049](https://doi.org/10.1109/SURV.2012.020212.00049).
- [15] Z. Zhou, M. Dong, K. Ota, J. Wu, and T. Sato, "Energy efficiency and spectral efficiency tradeoff in device-to-device (D2D) communications," *IEEE Wireless Commun. Lett.*, vol. 3, no. 5, pp. 485–488, Oct. 2014, doi: [10.1109/LWC.2014.2337295](https://doi.org/10.1109/LWC.2014.2337295).
- [16] Y. Cheng, C. Liang, Q. Chen, and F. R. Yu, "Energy-efficient D2D-assisted computation offloading in NOMA-enabled cognitive networks," *IEEE Trans. Veh. Technol.*, vol. 70, no. 12, pp. 13441–13446, Dec. 2021, doi: [10.1109/TVT.2021.3093892](https://doi.org/10.1109/TVT.2021.3093892).
- [17] L. Pei, Z. Yang, C. Pan, W. Huang, M. Chen, M. El-kashlan, and A. Nallanathan, "Energy-efficient D2D communications underlying NOMA-based networks with energy harvesting," *IEEE Commun. Lett.*, vol. 22, no. 5, pp. 914–917, May 2018, doi: [10.1109/LCOMM.2018.2811782](https://doi.org/10.1109/LCOMM.2018.2811782).
- [18] H. Sun, X. Chen, Q. Shi, M. Hong, X. Fu, and N. D. Sidiropoulos, "Learning to optimize: Training deep neural networks for interference management," *IEEE Trans. Signal Process.*, vol. 66, no. 20, pp. 5438–5453, Oct. 2018, doi: [10.1109/TSP.2018.2866382](https://doi.org/10.1109/TSP.2018.2866382).
- [19] K. Lee, J.-P. Hong, H. Seo, and W. Choi, "Learning-based resource management in device-to-device communications with energy harvesting requirements," *IEEE Trans. Commun.*, vol. 68, no. 1, pp. 402–413, Jan. 2020, doi: [10.1109/TCOMM.2019.2947514](https://doi.org/10.1109/TCOMM.2019.2947514).
- [20] S. Sharma and B. Singh, "Weighted cooperative reinforcement learning-based energy-efficient autonomous resource selection strategy for underlay D2D communication," *IET Commun.*, vol. 13, no. 14, pp. 2078–2087, Aug. 2019, doi: [10.1049/IET-COM.2018.6028](https://doi.org/10.1049/IET-COM.2018.6028).
- [21] E.-J. Han, M. Sengly, and J.-R. Lee, "Balancing fairness and energy efficiency in SWIPT-based D2D networks: Deep reinforcement learning based approach," *IEEE Access*, vol. 10, pp. 64495–64503, 2022, doi: [10.1109/ACCESS.2022.3182686](https://doi.org/10.1109/ACCESS.2022.3182686).
- [22] W.-J. Huang, Y.-W.-P. Hong, and C.-C.-J. Kuo, "Lifetime maximization for amplify-and-forward cooperative networks," *IEEE Trans. Wireless Commun.*, vol. 7, no. 5, pp. 1800–1805, May 2008, doi: [10.1109/TWC.2008.061075](https://doi.org/10.1109/TWC.2008.061075).
- [23] S. Landsburg, *Price Theory and Applications*. Gadag Road Hubballi, India: South-Western Pub., 2002, doi: [10.1142/13054](https://doi.org/10.1142/13054).
- [24] Q. Wu, G. Y. Li, W. Chen, and D. W. K. Ng, "Energy-efficient D2D overlaying communications with spectrum-power trading," *IEEE Trans. Wireless Commun.*, vol. 16, no. 7, pp. 4404–4419, Jul. 2017, doi: [10.1109/TWC.2017.2698032](https://doi.org/10.1109/TWC.2017.2698032).
- [25] L. Chen, J. Wu, H.-N. Dai, and X. Huang, "BRAINS: Joint bandwidth-relay allocation in multihoming cooperative D2D networks," *IEEE Trans. Veh. Technol.*, vol. 67, no. 6, pp. 5387–5398, Jun. 2018, doi: [10.1109/TVT.2018.2799970](https://doi.org/10.1109/TVT.2018.2799970).
- [26] J. Zhao, Q. Li, Y. Gong, Y. Ning, and F. Gao, "Price-based power allocation in two-tier spectrum sharing heterogeneous cellular networks," *J. Commun. Inf. Netw.*, vol. 3, no. 2, pp. 28–34, Jun. 2018, doi: [10.1007/s41650-018-0021-6](https://doi.org/10.1007/s41650-018-0021-6).
- [27] A. Tang, J. Wang, and S. H. Low, "Counter-intuitive throughput behaviors in networks under end-to-end control," *IEEE/ACM Trans. Netw.*, vol. 14, no. 2, pp. 355–368, Apr. 2006, doi: [10.1109/TNET.2006.872552](https://doi.org/10.1109/TNET.2006.872552).
- [28] J. Ding, L. Jiang, and C. He, "Energy-efficient power control for underlying D2D communication with channel uncertainty: User-centric versus network-centric," *J. Commun. Netw.*, vol. 18, no. 4, pp. 589–599, Aug. 2016, doi: [10.1109/JCN.2016.000082](https://doi.org/10.1109/JCN.2016.000082).
- [29] D. Liu, W. Wang, and W. Guo, "'Green' cooperative spectrum sharing communication," *IEEE Commun. Lett.*, vol. 17, no. 3, pp. 459–462, Mar. 2013, doi: [10.1109/LCOMM.2013.011113.121754](https://doi.org/10.1109/LCOMM.2013.011113.121754).
- [30] L. Lei, Z. Zhong, C. Lin, and X. Shen, "Operator controlled device-to-device communications in LTE-advanced networks," *IEEE Wireless Commun.*, vol. 19, no. 3, pp. 96–104, Jun. 2012, doi: [10.1109/MWC.2012.6231164](https://doi.org/10.1109/MWC.2012.6231164).
- [31] G. Araniti, A. Raschella, A. Orsino, L. Militano, and M. Condoluci, *Device-to-Device Communications over 5G Systems: Standardization, Challenges and Open Issues*. Berlin, Germany: Springer, 2017, pp. 337–360, doi: [10.1007/978-3-319-34208-5_12](https://doi.org/10.1007/978-3-319-34208-5_12).
- [32] A. A. Zaidi, R. Baldemair, V. Moles-Cases, N. He, K. Werner, and A. Cedergren, "OFDM numerology design for 5G new radio to support IoT, eMBB, and MBSFN," *IEEE Commun. Standards Mag.*, vol. 2, no. 2, pp. 78–83, Jun. 2018, doi: [10.1109/MCOMSTD.2018.1700021](https://doi.org/10.1109/MCOMSTD.2018.1700021).
- [33] M. Ahmed, A. Wahid, S. S. Laique, W. U. Khan, A. Ihsan, F. Xu, S. Chatzinotas, and Z. Han, "A survey on STAR-RIS: Use cases, recent advances, and future research challenges," *IEEE Internet Things J.*, vol. 10, no. 16, pp. 14689–14711, Aug. 2023, doi: [10.1109/JIOT.2023.3279357](https://doi.org/10.1109/JIOT.2023.3279357).
- [34] C.-H. Yu, K. Doppler, C. B. Ribeiro, and O. Tirkkonen, "Resource sharing optimization for device-to-device communication underlying cellular networks," *IEEE Trans. Wireless Commun.*, vol. 10, no. 8, pp. 2752–2763, Aug. 2011, doi: [10.1109/TWC.2011.060811.102120](https://doi.org/10.1109/TWC.2011.060811.102120).
- [35] T. Wang, A. Cano, G. B. Giannakis, and J. N. Laneman, "High-performance cooperative demodulation with decode-and-forward relays," *IEEE Trans. Commun.*, vol. 55, no. 7, pp. 1427–1438, Jul. 2007, doi: [10.1109/TCOMM.2007.900631](https://doi.org/10.1109/TCOMM.2007.900631).
- [36] S. Boyd and L. Vandenberghe, *Convex Optimization*. Cambridge, U.K.: Cambridge Univ. Press, 2004, doi: [10.1198/jasa.2005.s41](https://doi.org/10.1198/jasa.2005.s41).
- [37] A. Schrijver, *Theory of Linear and Integer Programming* (Wiley-Interscience Series in Discrete Mathematics and Optimization). Hoboken, NJ, USA: Wiley, 1999, doi: [10.2307/253980](https://doi.org/10.2307/253980).
- [38] H. Zhu, M. Zhou, and R. Alkins, "Group role assignment via a Kuhn-Munkres algorithm-based solution," *IEEE Trans. Syst., Man, Cybern., A, Syst. Hum.*, vol. 42, no. 3, pp. 739–750, May 2012, doi: [10.1109/TSMCA.2011.2170414](https://doi.org/10.1109/TSMCA.2011.2170414).
- [39] W. A. McEachern, *Microeconomics: A Contemporary Introduction*. Cincinnati, OH, USA: South-Western College Pub., 2005.
- [40] Y. Yu, W. Zhang, X. Zhang, W. Wang, and C. Wang, "Hierarchical spectrum sharing for cognitive radio networks based on microeconomic theory," in *Proc. IEEE 24th Annu. Int. Symp. Pers., Indoor, Mobile Radio Commun. (PIMRC)*, Sep. 2013, pp. 1–5, doi: [10.1109/PIMRC.2013.6666530](https://doi.org/10.1109/PIMRC.2013.6666530).



YANG YU received the B.S., M.S., and Ph.D. degrees in electronic information engineering from the Beijing University of Posts and Telecommunications, Beijing, China, in 2009, 2011, and 2014, respectively. He is currently an Associate Professor with the Electronic Information School, Hubei Three Gorges Polytechnic. He is the author of more than ten articles. He holds five patents. His current research interests include energy harvesting, artificial intelligence, and D2D communication.



XIAOQING TANG received the B.S., M.S., and Ph.D. degrees in electronic information engineering from Wuhan University, Wuhan, China, in 2010, 2012, and 2015, respectively. He is currently an Associate Professor with the School of Artificial Intelligence, Hubei University. He is the author of more than ten articles. He holds three patents. His current research interests include the IoT circuit and systems, RF energy harvesting, and backscattering communication.

• • •